Radiation Measurements 191 (2026) 107588

Contents lists available at ScienceDirect

Radiation Measurements

journal homepage: www.elsevier.com/locate/radmeas

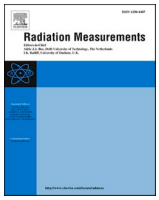

TL/OSL emission spectrometry of alumina substrates of electronic components in mobile phones: potential of the red TL emission for retrospective dosimetry

Clemens Woda [a,b,*], Michael Discher [a,c]

[a] Helmholtz Zentrum München, Institute of Radiation Medicine, Ingolstädter Landstraße 1, 85764, Neuherberg, Germany
[b] Federal Office for Radiation Protection (BfS), Ingolstädter Landstraße 1, 85764, Neuherberg, Germany
[c] Paris-Lodron-University of Salzburg, Department of Environment and Biodiversity, 5020, Salzburg, Austria

ARTICLE INFO

Keywords:
TL/OSL emission spectrometry
Retrospective dosimetry
Emergency dosimetry
Alumina substrates of resistors and inductors
Red thermoluminescence
Mobile phones

ABSTRACT

Emergency dosimetry using mobile phone components has become an increasingly interesting field for post-accident dose assessment. This study investigates the TL and OSL emission properties of alumina substrates from resistors and inductors found in mobile phone circuit boards, with a focus on the dosimetric potential of the red Cr^{3+}-related TL emission. Spectral measurements reveal three primary emission bands around 330 nm and 410 nm, attributable to F^+ and F centers respectively, and a dominant emission at 695 nm, characteristic of Cr^{3+}. In TL, the Cr^{3+} emission clearly dominates, particularly in resistors, with intensity exceeding that of the blue/UV emissions by up to two orders of magnitude. The red TL signal exhibits a linear dose response over a wide range (from mGy to >10 Gy), low intrinsic background, and fading characteristics consistent with anomalous fading (~20.7 %/decade). Dose recovery experiments immediately after irradiation confirm accuracy within 7 %, a minor dose overestimation caused by minor desensitization. The red TL signal is optically bleachable, similar to its blue/UV counterpart. Irradiation trials with intact smartphones demonstrated that the red TL method delivers dose estimates within 25 % of the reference dose, comparable to established methods using display glass or OSL on resistors. Importantly, dose estimation using only a single resistor achieved similar sensitivity to protocols requiring ten components in the blue/UV range. These results highlight the potential of red TL for accurate, sensitive, and minimally invasive retrospective dosimetry. The method offers distinct advantages in scenarios where only few components are available and enables the prospect of non-destructive measurements.

1. Introduction

Emergency dosimetry using personal objects carried on or close to the human body has received increasing attention in the last 15 years due to the constant threat or risk of unplanned exposure of the general population with ionizing radiation, either due to radiation accidents or malevolent use of ionizing radiation. Mobile phones, being widespread among the population, seem to be particularly promising in this respect and therefore many electronic materials found in the phones, either as part of the display or on the circuit board, have been the subject of several investigations: Touchscreen glass of modern smartphones using EPR (Fattibene et al., 2014), TL or PTTL (Discher et al., 2016; McKeever et al., 2017), display glass using TL (Mrozik et al., 2014; Discher et al., 2013; Bassinet et al., 2010), screen protectors (Discher et al., 2023; Bassinet et al., 2022; Bassinet and Le Bris, 2020), integrated circuits (IC) using OSL (Mrozik et al., 2017; Sholom and McKeever, 2016), Inductors using OSL or TL (Bassinet et al., 2017; Fiedler and Woda, 2011; Lee et al., 2017) and most notably resistors, using OSL or TL (Ademola and Woda, 2017; Inrig et al., 2008). For the latter two materials, the radiation sensitive part is the alumina substrate, used to construct the components.

While luminescence properties of some materials seem to vary and no consolidated picture has yet emerged, luminescence dosimetry using OSL on resistors has reached a certain level of maturity and standardization, with several papers independently confirming the main dosimetric properties and a “fast mode” and “full mode” protocol having been validated in an inter-laboratory comparison (Bassinet et al., 2014). The dose assessment method has also been tested in realistic accident

* Corresponding author. Federal Office for Radiation Protection, Ingolstädter Landstraße 1, 85764, Neuherberg, Germany.
E-mail address: cwoda@bfs.de (C. Woda).

https://doi.org/10.1016/j.radmeas.2025.107588
Received 5 August 2025; Received in revised form 13 November 2025; Accepted 8 December 2025
Available online 8 December 2025

scenarios, involving a sealed Ir-192 source, placed either in a bus (Discher et al., 2021; Rojas Palma et al., 2020) or in front of different arrangements of anthropomorphic phantoms (Kim et al. 2022, 2025; Waldner et al., 2021). The dose response of the OSL (UV detection window) and TL (blue detection window) signals of resistors is linear up to at least several Gy (Ademola and Woda, 2017; Lee et al., 2017; Inrig et al., 2008). Both signals are not stable at room temperature but follow the characteristic decay pattern of anomalous fading, with a signal loss of about 50 % after 10 days storage (ibid.). The detection limit varies according to the luminescence reader characteristics (e.g. stimulation power for OSL), amount of sample material (number of resistors of a given size, variation of radiation sensitivity between resistors) and time passed between measurement and exposure. For resistors of size 1 x 0.5 $\times$ 0.35 mm^3 (L x W x H, code 0402) and ~35 mW cm^{-2} stimulation power, detection limits for OSL have been reported from ~10 mGy immediately after irradiation for 10 components to ~50 mGy for measurement 10–20 days after exposure and 20 components (Geber-Bergstrand et al., 2018; Discher et al., 2021). For the TL method on the same material, a detection limit of 50 mGy has been assessed, when using 10 resistors of size code 0402 (Ademola and Woda, 2017). In this case, the detection is not limited by the measurement sensitivity but by the presence of intrinsic background signals of variable shapes and intensities, sometimes also called zero-dose or native signals.

OSL decay curve shape and shape and position of the main TL peaks (measured in the UV or blue detection window) of the alumina substrates of resistors are similar to Al_2O_3:C, for which the emission properties and responsible defects are well understood (Yukihara and McKeever, 2011). Lee et al. (2017) showed in a preliminary TL emission spectrometry study, that for both resistors and inductors, an intense emission peaking at 700 nm is seen, which the authors tentatively ascribed to Cr^{3+} impurities, with additional weaker broad emissions between 300 and 500 nm, that could not be separated into individual peak signatures.

The aims of the present study are twofold. First to re-investigate the TL emission spectra of inductors and resistors, with higher resolution for a more detailed analysis and complemented by OSL emission spectra to independently confirm, complement and refine the results of Lee et al. (2017). And secondly to investigate the dosimetric properties and potential of the red TL emission of resistors for retrospective dosimetry.

2. Materials and methods

Investigations were carried out on resistors and inductors extracted from the circuit boards of several mobile phones and from sample kits obtained from AGL Technology GmbH (Producer: YAGEO). Sample preparation was carried out under subdued red light conditions to avoid phototransfer from deeper traps (Ademola and Woda, 2017). The electronic components were cleaned in an ultrasonic bath with acetone for about 15–20 min to remove the adhesive used to secure the components to the circuit board during the process of manufacturing. For spectral measurements, twenty resistors or inductors were placed with the ceramic side facing upwards on a stainless-steel cup sprayed lightly with silicon. For PMT measurements, the number of components varied between one to ten. For resistors and inductors the individual component size was always 0402 (1 x 0.5 $\times$ 0.35 mm^3 (L x W x H)).

For trial irradiations, two intact mobile phones were irradiated in kerma reference conditions with a dose of 1 Gy (air kerma value) using a Cs-137 source of the irradiation facilities of the Helmholtz Zentrum München. The distance of the circuit board within the mobile phones to the source was 1 m, with the front side of the phone (cover glass) facing the source and attached to a 2 mm thick Perspex layer, used for build-up. One of the phones was additionally equipped with reference dosimeters: Thin-layer LUXEL® detectors were fixed at an approximately central position to the front side of the phone, between the circuit board and battery and on the backside of the phone. In addition, two pieces (approx. 5 $\times$ 5 mm^2) of thermally annealed display glass (reference glass) were taped onto the front side of the phone, towards the top and the bottom of the phone display. After irradiation, the mobile phones were disassembled in the laboratory (under dark room conditions), electronic components extracted, cleaned, dried and placed onto the measuring cup. Three cups per phone were prepared, the first one with 4–5 resistors and the second with a single resistor for measurements using TL and the third one with 10 resistors for measurements with OSL using the "fast mode" protocol described in Bassinet et al. (2014). Two pieces of display glass per phone were also prepared, one without and one with etching in 40 % HF for 4 min (Discher et al., 2013). Glass samples (reference and display glass) were measured using the "pre--bleached with blue LEDs" protocol (Discher et al., 2013; Discher and Woda, 2013). LUXEL detectors were measured using the protocol described in Discher et al., (2021).

TL measurements in the red spectral range were carried out with a Freiberg Instruments Lexsyg research luminescence reader (Richter et al., 2013) equipped with an in-built $^{90}Sr/^{90}Y$ β-source. For measurements, a combination of a Schott OG570 longpass glass filter and a Schott KG 3 glass filter, each with 3 mm thickness, in combination with a thermo-electrically cooled Hamamatsu H7421-40 GaAsP PMT was used. The latter has a spectral response of 300–720 nm, and an efficiency at 700 nm of around 20 % of the peak efficiency. A heating rate of 2 °C s^{-1} was used and samples were preheated at 120 °C for 10 s in order to remove the lower temperature TL peak at ~80 °C, to be discussed further below and also shown in TL measurements of the blue/UV emissions (Woda et al., 2010; Beerten et al., 2009). TL measurements were conducted twice on the same cup and the second measurement subtracted from the first to remove the background due to thermal radiation. Unless stated otherwise, the TL glow curves were integrated from 125 °C to 180 °C for data analysis (see sections 3.2.1 and 3.2.2). For the fading experiment, described in section 3.2.4, a single aliquot of 5 resistors was used. Before the first irradiation, the sample was first thermally annealed up to 400 °C and then subjected to a total of fourteen cycles of irradiation-storage (at room temperature for a certain time) – readout. After each cycle, the TL response to a fixed test dose (0.8 Gy) was monitored and the TL fading signal normalized to this test dose signal, to correct for any possible sensitivity changes. In addition, the storage time was not increased systematically but changed in a random manner during the experiment (e.g. no storage, then 3 h storage, then 5 min, then 4 days, then 20 min etc.). In this way any possible systematic change in fading characteristics with repeated cycles of irradiation and measurement will only produce a larger scatter of data points but not a systematic bias in the derived results.

OSL measurements of resistors and LUXEL detectors and TL measurements of the reference and display glasses were carried out on a Risø TL/OSL DA15 automated reader, equipped with blue LEDs (470 ± 30 nm, 36 mW cm^{-2}) for stimulation and a Thorn-EMI 9235 bialkali photomultiplier combined with a 7.5 mm U-340 Hoya filter (290–370 nm) for detection. The in-built $^{90}Sr/^{90}Y$ β-sources of both readers, Lexsyg research and Risø TL/OSL DA15, were cross-calibrated for each material (resistor substrates, LUXEL detectors, display glass) against the Cs-137 source described further above using samples of each material irradiated in kerma reference conditions.

TL and OSL emission spectra were recorded using the emission spectrometry unit of the Lexsyg research reader, consisting of a thermo-electrically cooled Andor Technology iDus 420 Series CCD camera, operating at -80 °C, and a Shamrock 163 spectrometer. TL spectra in the wavelength range of 300–800 nm were recorded with a heating rate of 2 °C s^{-1} and an integration time of either 5 s (for 3D plots) or 20 s (for detailed spectral analysis), OSL spectra using green diodes, with 35 mW cm^{-2} stimulation power at the sample position, an integration time of 20 s and a combination of a Schott BG3 (3 mm thickness) and an Edmund Optics OD4 525 nm shortpass filter. With this filter combination a useable detection window of 300 nm–~470 nm is possible as opposed to a reduced detection window of 330 nm–~470 nm, when using the standard combination of a Schott BG3 and BG39 glass filter,

originally supplied with the reader. This advantage is slightly offset by an insufficient blocking of photoluminescence signals for higher wavelengths, leading to a non-constant, sample and exposure time dependent background in the region of interest. For background subtraction, the last frame of the series of OSL spectral measurements was used (60–80 s) and a straight line fitted to the parts of the spectrum in the region of interest that is unaffected by any remaining signal (see Fig. 1). All spectral measurements were corrected for the spectral response of the system, i.e. the combined, wavelength-dependent efficiency of the different components of the spectrometer (optical glass fiber, grating, camera, filter transmission), using a Bentham Instruments Ltd. Calibration irradiance standard lamp (Type: CL 6). For fitting of TL and OSL spectra with Gaussian shaped emission bands, data were corrected for unequal spacing with regard to photon energy by multiplying the intensity with $\lambda^2/(h\,c)$ (Blasse and Grabmaier, 1994).

3. Results and discussion

3.1. TL/OSL emission spectra

The TL emission spectra of a cup of 10 resistors and of a cup of 10 inductors, both taken from the sample kits, is shown as 3D isometric and contour plots in Fig. 2. Similar spectra were observed for electronic components taken directly from mobile phones. For resistors a single dominant emission with a sharp peak at 695 nm is seen, with two TL peaks at around 200 °C and 330 °C. The peak temperatures are similar to the ones reported for TL glow curves of resistors, measured in the blue wavelength range (Ademola and Woda, 2017). For inductors, the same dominant emission in the red is visible but also a blue emission peaking at 420 nm. Again, two TL peaks are observed for both emissions, with somewhat lower peak temperature compared to resistors but which fit the reported TL glow peaks for inductors in the literature, measured in the blue wavelength range (Fiedler and Woda, 2011). Since the TL spectral measurements have a comparatively coarse temperature resolution of 10 °C and have been interpolated for the purpose of plotting, peak temperatures inferred from the spectra should only be taken as approximative. The TL spectra are in good agreement with the ones reported in Lee et al. (2017) for the same material, confirming the results

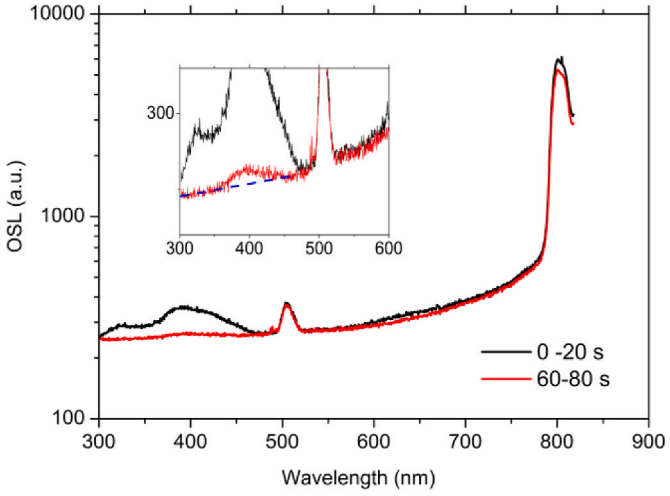

Fig. 1. Illustration of the procedure for background correction for measurements of OSL spectra. An enlargement of the area from 300 to 600 nm on a linear scale is shown in the inset. The blue dashed line indicates the linear fit to the parts of the OSL spectrum (red line) without signal. The peak at ~504 nm is breakthrough light of the stimulating LEDs, the strong peak at 807 nm breakthrough of photoluminescence signals from the sample. The spectrum shown here has been cleaned of cosmic ray peaks but otherwise is as-measured and uncorrected. (For interpretation of the references to colour in this figure legend, the reader is referred to the Web version of this article.)

of the latter work.

A more detailed analysis of the emission spectra in selected temperature regions is shown in Fig. 3, measured with a lower temperature resolution (40 °C) and, for resistors, also with a higher dose, to increase the signal to noise ratio. In the temperature interval 140–180 °C for resistors now also the existence of additional emissions in the blue/violet wavelength range (2.5–4 eV, 300–500 nm) is visible, but at intensities of about 100 times less than the red emission, similar to the observations in Lee et al. (2017). The original wavelength resolution of the spectral measurement now also reveals a more detailed structure of the red emission, which is the same as the well-known Cr^{3+} emission (Ibarra et al., 1991). The emission region at lower wavelengths (higher photon energies) can be well fitted by the sum of two Gaussian shaped emission bands (Fig. 3c), with central energies around 2.9 and 3.8 eV (corresponding to about 430 and 330 nm). The same holds true for the corresponding OSL spectrum (Fig. 3e). For inductors and the lower temperature TL peak also two emission bands are necessary for fitting the blue/violet wavelength range (Fig. 3b), although the emission at ~2.9 eV is clearly dominating, similar to the OSL spectrum of the same sample (Fig. 3f), whereas for the higher temperature peak a single emission at 2.9 eV is sufficient for a good fit to the measured spectrum.

For comparison, the TL and OSL emission spectrum was also measured for dosimetry-grade chip of Al_2O_3:C (TLD-500) and shown in Fig. 4. These crystals are grown in a reducing atmosphere, catalysing oxygen-vacancy center production and the crystals have high F-center concentrations (oxygen vacancy with two electrons) and lower concentrations of F^+-centers (oxygen vacancy with a single electron; Akselrod et al., 1998). At sufficiently high doses, the luminescence emissions from both centers can be seen and the spectrum well decomposed into the two emission bands. The signature of the Cr^{3+} emission can also be seen but at much lower (relative!) intensity due to the synthesis process. The summary of all fitting results is given in Table 1. For Al_2O_3:C, the values of the central energy for the two emissions of about 3.0 and 3.7 eV (413 and 335 nm) are close to the ones reported for the F and F^+ centers in the literature and therefore also confirm the validity of the fitting approach (in combination with the wavelength and efficiency calibration of the spectrometric system). The wavelengths corresponding to the central energies of the two emission bands for resistors and inductors lie in a very similar range (400–420 nm and 320–330 nm), indicating that these too could be F and F^+ centers in the alumina substrates. The fitting results also show that the width of the two emissions is significantly larger in alumina substrates that in Al_2O_3:C, which is reasonable, considering that the former is a polycrystalline, disordered material, compared to the single crystal nature of the latter. For resistors this implies that while in TL a separate measurement of only the F center (420 nm) emission can be achieved by suitable optical filters, the opposite (a detection of a pure F^+ center emission) is more difficult to realize. For OSL, in particular, the standard configuration of using blue LEDs for stimulation and a Hoya U-340 optical filter for detection (290–370 nm) will always measure a mixture of both emissions. From Fig. 3 it can also be seen that the intensity ratio of the (presumably) F^+ to F emission in resistors and inductors decreases with temperature, from the largest at room temperature (OSL spectra) to below detection limit for inductors above 240 °C. It is known that the emission of both the F and F^+ center is subjected to thermal quenching (Akselrod et al., 1998; Evans and Stapelbroek, 1978). The observed intensity decrease could thus be the result of a stronger thermal quenching of the F^+ emission compared to the F emission in alumina substrates.

The analysis also revealed an unequivocal assignment of the 695 nm emission to the (R-line) emission of Cr^{3+}. Chromium is a ubiquitous impurity in nearly all forms of Al_2O_3 and is characterised by absorption bands at 400 nm and 550 nm (McKeever et al., 1999). The significance of the first band is that it efficiently absorbs the 420 nm luminescence (and to a lesser degree also the 330 nm emission), which through relaxation in turn leads to an additional 695 nm emission. A high Cr^{3+} concentration thus leads to an enhanced 695 nm emission at the expense of a

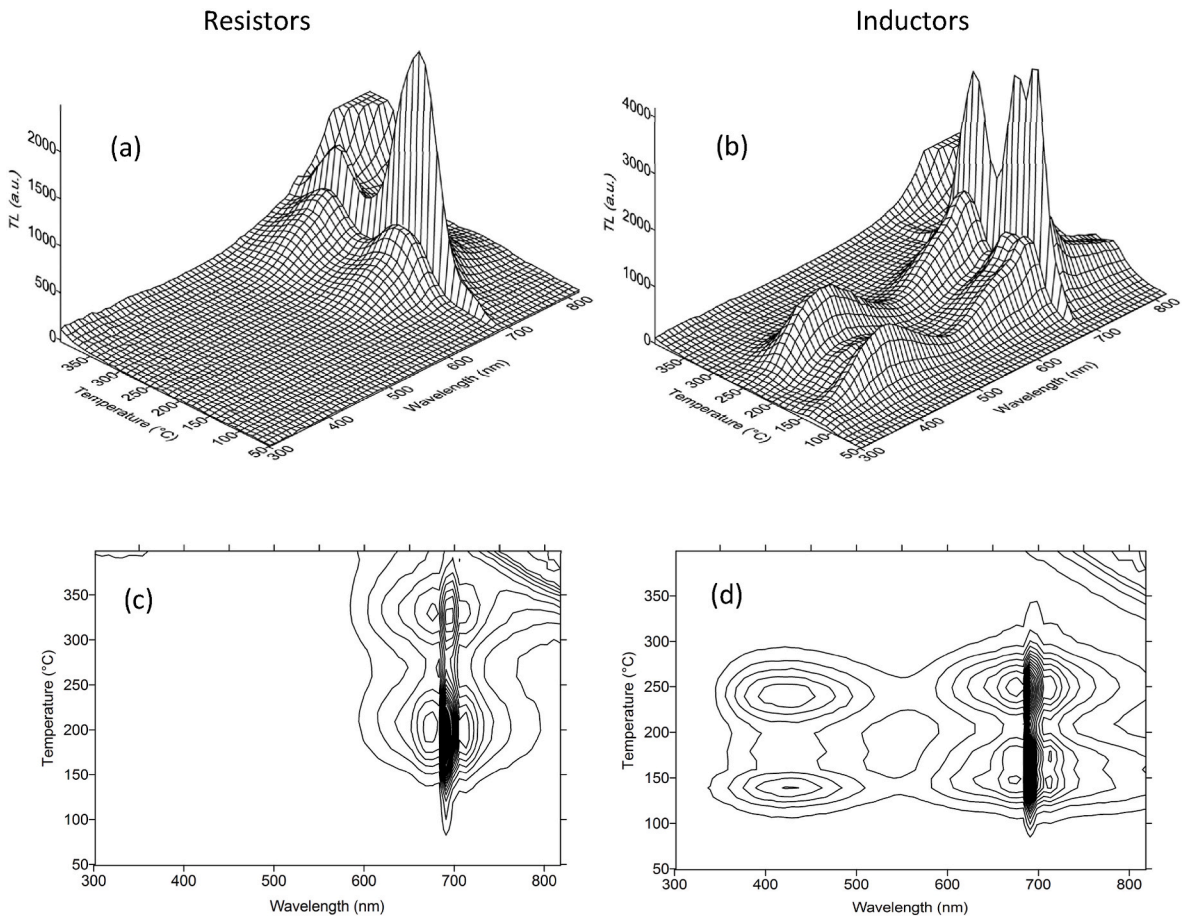

Fig. 2. TL Spectra of resistors and inductors. The panels on the left (a and c) show the spectrum for 10 resistors, irradiated with 100 Gy, the panels on the right (b and d) for 10 inductors, irradiated with 900 Gy. (a) and (b) are the isometric plots, (c) and (d) the respective contour plots. Spectra were taken at 10 °C temperature intervals and interpolated for plotting. The apparent double peak for the ~150 °C emission for inductors is an artefact of the temperature interpolation.

(suppressed) emission from F and F^+ centers by self-absorption in the material. This and the experimental fact of the extreme dominance of the Cr^{3+} emission in the TL spectrum of resistors prompted the investigations of the dosimetric properties of this emission for retrospective dosimetry using a suitable detector and filter.

3.2. Dosimetric properties of the Cr^{3+}-emission of resistors

3.2.1. Detection window, glow curve and dose response

The comparison of the chosen detection window, determined by the sensitivity of the red enhanced PMT and the combination of optical filters used (Schott OG570 and KG3), with the TL emission spectrum of resistors is shown in Fig. 5 (panel A). As can be seen, emissions below 550 nm are effectively suppressed while the major part of the rising flank of the red emission and to a minor degree also the 695 nm peak itself is picked up. The enhanced sensitivity in the red wavelength range comes at the expense of a strongly increased background due to thermal radiation at higher temperatures, when measuring a TL glow curve (Fig. 5, panel B). This limits the measurable range with the reader employed in this study to 400 °C and even above 260 °C, sensitivity becomes increasingly reduced due to an enhanced noise level (as a result of subtracting two very high thermal radiation background signals). On the other hand, the level of dark current of the PMT remains constant up to about 200 °C, which encompasses the relevant range for signal integration in this study (see further below).

A typical TL glow curve of resistor substrates measured with the setup is shown in Fig. 6 (panel A). Next to the TL peaks at 180 °C and 320 °C, already described in the context of the spectral measurements (but determined here with a sufficient temperature resolution), there is an additional low temperature peak at ~80 °C. Since samples were preheated to remove the 80° peak, the lower integration limit of the dosimetric signal (180° peak) could be set to 125 °C. The upper limit of 180 °C is motivated in the next section. Glow curve shape and peak positions are similar to the ones measured in the blue wavelength range (Ademola and Woda, 2017; Woda et al., 2010; Inrig et al., 2008). For resistors taken from the sample kit and measured in Fig. 6 (panel B), the dose response of the 180 °C peak is linear in the dose range from tens of mGy to tens of Gy, with good reproducibility, whereas the dose response of the 320 °C peak is supralinear with evidence of sensitization.

3.2.2. Intrinsic background signals

When performing TL measurements on unexposed samples, non-radiation induced signals are observed in the relevant temperature range (called intrinsic background signals, native signals or zero-dose signals, Fig. 7, panel A). There is a certain similarity in shape between the signals of the investigated samples, with moderate signal levels up to around 180°-200 °C and a pronounced increase in signal intensities for higher temperatures. As a result, the upper integration limit for the dosimetric signal was set to 180 °C in this study. With this integration range, the intrinsic background signals can be converted to (apparent) intrinsic background doses, after calibration, this is shown in panel B of Fig. 7. For the twelve measured samples, the apparent intrinsic doses vary between ~1 and 10 mGy. This is substantially lower than what has been reported for measurements of resistors in the blue wavelength range (up to 80 mGy; Ademola and Woda, 2017) and can be seen as an additional advantage of the different detection window. Nevertheless,

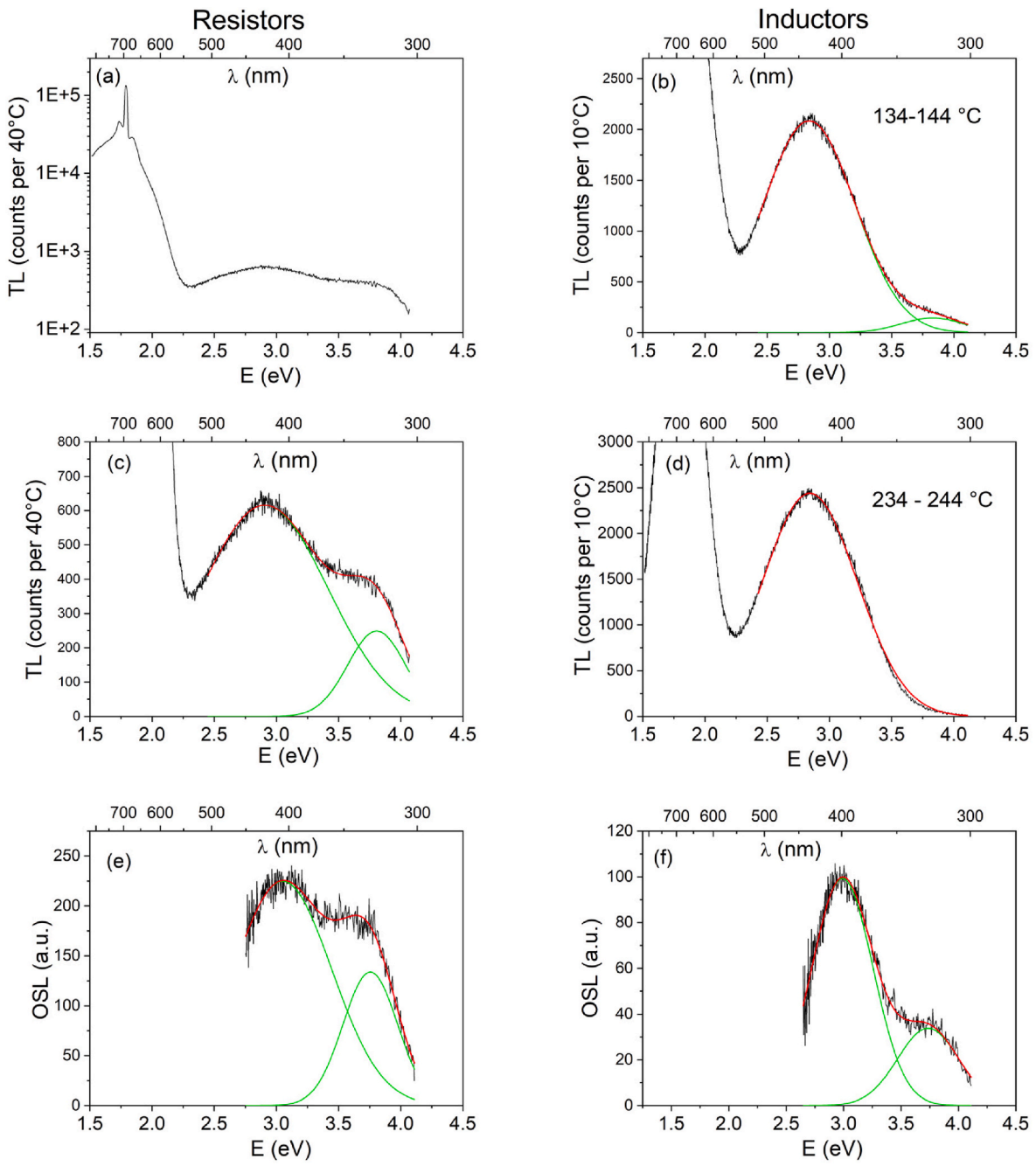

Fig. 3. Panels on the left (a, c, e) display TL and OSL spectra of resistors, panels on the right (b, d, f) TL and OSL spectra of inductors. Irradiation dose was always 900 Gy. For resistors, the TL spectrum is shown in the temperature interval 140–180 °C (a+c), and for OSL the spectra of nine cups, containing 10 irradiated components each, was added to improve the otherwise very low signal to noise ratio (e). For inductors, two TL spectra are shown in the temperature intervals 134–144 °C (b) and 234–244 °C (d), for the two separate TL peaks visible in Fig. 2. Also shown is this the deconvolution of the blue/UV region into Gaussian shaped emission bands (green lines) for all spectra. (For interpretation of the references to colour in this figure legend, the reader is referred to the Web version of this article.)

the existence of the intrinsic background signals has implications for the minimum measurable doses. On thermally annealed samples, a detection limit of 0.2–0.6 mGy can be estimated using the radiation sensitivity and three standard deviations of the background, the exact values depending on the number of components used per measuring cup (3–8 for the samples of Fig. 7). The presence of the intrinsic background signals increases the detection limit in practical terms to several mGy.

3.2.3. *Reproducibility and dose-recovery tests in the reader*

The reproducibility of a TL measurement was investigated for resistors taken from two different mobile phones of the same brand, by performing several cycles of irradiation with 0.8 Gy, preheat and readout (Fig. 8). A minor but continuous decrease in TL response is observed, with the largest change occurring in the very first irradiation-readout step (drop of 5 and 12.5 %, respectively). For subsequent cycles, the rate of decrease is reduced with the signal intensity being around 10 % lower after 10 cycles, compared to the second cycle. This gradual apparent de-sensitization was not observed for the sample in Fig. 6. One possible reason could be that in Fig. 6, resistors from the sample kit were measured, which do not require cleaning, whereas in Fig. 8, resistors from actual phones were used, that were cleaned in acetone prior to measurement to remove glue residues. Possibly the cleaning procedure

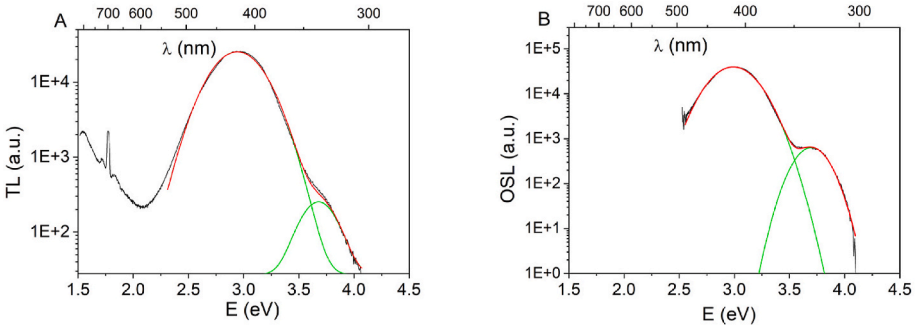

Fig. 4. Comparative TL and OSL spectrum of an Al_2O_3:C chip, irradiated either with 500 Gy (TL, Panel A), in the temperature interval of 164–168 °C or with 100 Gy (OSL, Panel B), in the time interval of 0–2s.

Table 1
Compilation of the fitting parameters of the TL and OSL emissions 1 and 2 of resistors, inductors and Al_2O_3:C. Given are the central energy (E) and the full width at half maximum (FWHM). For the third emission, the read off energy of the main sharp peak is also given.

Technique	Material	Emission 1		Emission 2		Emission 3
		E (eV)	FWHM (eV)	E (eV)	FWHM (eV)	E (eV)
TL	Resistors	2.91	1.02	3.80	0.46	1.79
TL	Inductors	2.84	0.74	3.83	0.51	1.79
TL	Al_2O_3:C	2.94	0.5	3.68	0.34	1.79
OSL	Resistors	3.05	0.79	3.75	0.44	
OSL	Inductors	2.99	0.53	3.74	0.53	
OSL	Al_2O_3:C	2.99	0.36	3.70	0.26	

was not completely effective leading to the observed de-sensitization. On the other hand, the test in Fig. 8 was carried out for a single dose and the degree of sensitivity change might also be dose dependent. Clearly, more experiments are needed for improving sample preparation and measurement of dose response.

To investigate the performance of a dose measurement in ideal conditions, given the current sample preparation and measurement protocol, dose-recovery tests were carried out, irradiating and measuring the sample in the same reader without time delay. All samples were first preheated to 230 °C, to remove any pre-existing zero-dose signals in the relevant signal integration range. Number of resistors per sample varied between four and eight. Given dose was 0.8 Gy and three dose points were used for calibration, bracketing the expected dose with an additional recycling step of the lowest dose points added at the end of the measurement sequence (four cycles in total for the calibration curve). The results are shown in Fig. 9. In line with the de-sensitization observed in Fig. 8, a minor but significant dose overestimation can be seen. The average ratio of measured to given dose amounts to 1.07 ± 0.02. The recycling ratios for all samples was consistently lower than 1 with an average of 0.94 ± 0.02. Considering that the latter corresponds to the intensity ratio of the fifth to the second irradiation-measurement cycle, with the first cycle corresponding to the measurement of the simulated accident dose, this average recycling ratio is similar to the sensitivity decrease in Fig. 8. For test purposes, the average sensitivity decrease for each cycle of Fig. 8 was calculated (between cycles two and five) and used to correct the calibration curves of the dose-recovery test of Fig. 9. An example of this procedure is given in Fig. 10. With these "sensitivity corrected" calibration curves the average ratio of measured to given dose and the average recycling ratio change to 1.038 ± 0.002 and 1.00 ± 0.02, respectively. This implies that of the ~7 % dose overestimation, 4 % can be tentatively ascribed to the sensitivity change due to the measurement of the simulated accident signal and 3 % to the de-sensitization during measurement of the calibration curve. Generally, the overall degree of overestimation does not seem to be critical when considering the many additional large uncertainties in emergency dosimetry. Nevertheless, improvements to reduce the dose overestimation could be investigated in further studies. On the other hand, the effect is smaller than what has been found for measurements in the blue wavelength range, where a systematic dose overestimation of around 40 % has been determined (Ademola and Woda, 2017).

3.2.4. Optical stability and fading

In both Woda et al. (2010) and Inrig et al. (2008) it has been shown that the dosimetric TL peak at 190 °C, measured in the blue or UV wavelength range, is optically sensitive and can be reduced in intensity by blue light stimulation, with the peak temperature shifting towards higher temperatures for increasing stimulation times. A very similar observation can be made for the red TL, with stimulation times of the blue LEDs ranging up to 1000 s (Fig. 11). Finally, the fading characteristics of the Cr^{3+} emission was analyzed in a preliminary experiment, using 5 resistors extracted from a single smartphone, by irradiation with 0.8 Gy and storage at room temperature and in the dark for different time periods before measurement (Fig. 12). Signals were normalized to a test-dose response and the storage time was increased in a random manner (see section 2 for details). The decrease of signal intensity with time follows the well-known functional behavior for anomalous fading, for which Huntley and Lamothe (2001) have introduced the following functional relationship:

$$I = I_C\left[1 - \frac{g}{100}\cdot\log_{10}\left(\frac{t}{t_C}\right)\right],$$

where I_C is the luminescence intensity at some time t_C following irradiation and g is the percent decrease in intensity per decade. For comparison with published values, the same t_C = 8.3 h was used as in previous publications. This resulted in a g value of 20.7 % per ten-fold increase in t_C, a value which lies in a similar range as the g values reported for the blue emission at different temperature integration intervals (ranging from 100-150° to 100–200 °C) in Ademola and Woda (2017) and which is smaller than the fading rate of the OSL signal (Ademola and Woda, 2017; Inrig et al., 2008). The similarities in glow curve shape, linearity of dose response, optical stability and fading characteristics of the red and blue/UV emissions indicate that it could be the same trap(s) that is(are) feeding the different recombination centers. Whether this is a hole or an electron trap, or whether electrons and holes are released from different traps at the same temperature cannot be decided from the data presented.

3.2.5. Trial irradiations

For a first evaluation of the potential of the red TL of resistors for retrospective dosimetry an irradiation trial using two intact phones and a Cs-137 source, described in section 2, was carried out. Measurements were carried out 15 days after irradiation and for one phone (LG P700) also 4 h after irradiation on an additionally prepared set of sample material. For calibration of the red TL signal in the reader, the same

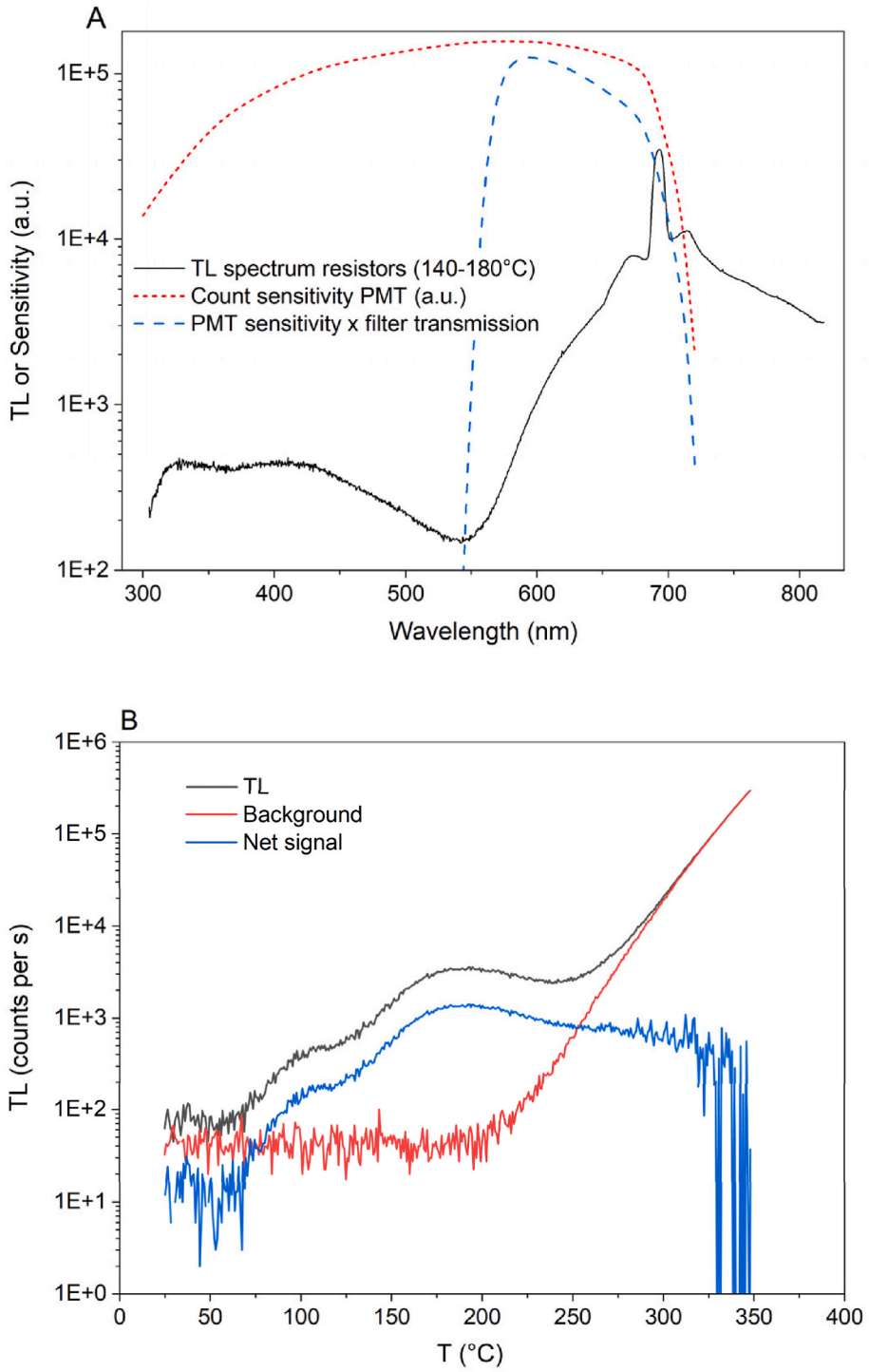

Fig. 5. Panel A: Comparison of the TL spectrum from resistors (in the temperature region 140–180 °C; black solid line) with the count sensitivity of the employed PMT (red short dashed line) and with the combination of PMT sensitivity and optical transmission of the glass filters used (blue dashed line). The TL spectrum is given here in its originally measured form with respect to wavelength, therefore doesn't need to be corrected for unequal x-data spacing and thus displays somewhat different relative intensities between red and blue/UV emission than the spectrum shown in Fig. 3 (a). Panel B: Example glow curves of a first ("TL", black line) and second ("Background", red line) TL measurement of an irradiated resistor sample with the setup of panel A. "Net signal" is the difference between the two measurements. (For interpretation of the references to colour in this figure legend, the reader is referred to the Web version of this article.)

approach as for dose recovery tests in the reader (section 3.2.3) was used: three dose points, bracketing the expected dose with an additional recycling step of the lowest dose points added at the end of the measurement sequence. For resistors from the LG phone model, the average recycling ratio was 0.98 ± 0.01 and for resistors from the Samsung model, 0.88 ± 0.03. Resistors from the former sample thus showed negligible change in red TL sensitivity, whereas for the latter a somewhat stronger de-sensitization than the one shown in Fig. 8 occurred. Results of the different dose assessment methods are shown in Fig. 13. LUXEL detectors indicate a small but noticeable dose gradient trough the phone sample, with the detectors on the front and close to the circuit board agreeing well in dose value with the reference glass and the set air

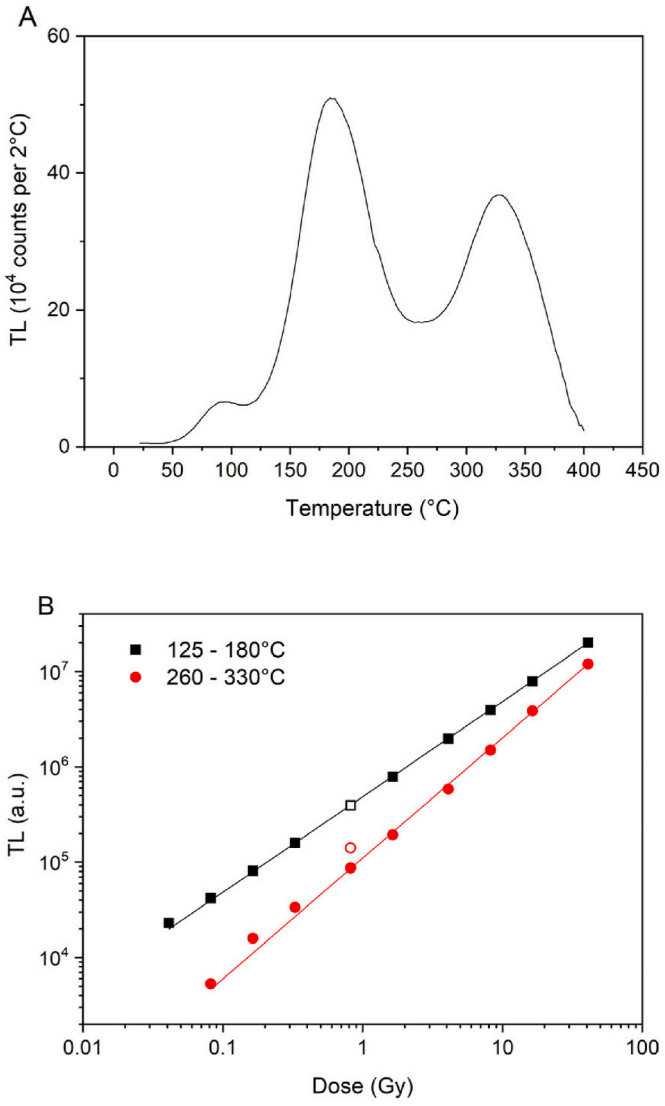

Fig. 6. Upper panel A: Red TL Glow curve of 10 resistors from a Samsung Galaxy 3 after irradiation with 10 Gy. Lower panel B: Dose response of the Cr^{3+} emission in two integration ranges: 125–180 °C (black square symbols) and 260–330 °C (red circle symbols, intensity divided by a factor of 3); 20 resistors taken from the sample kit. (For interpretation of the references to colour in this figure legend, the reader is referred to the Web version of this article.)

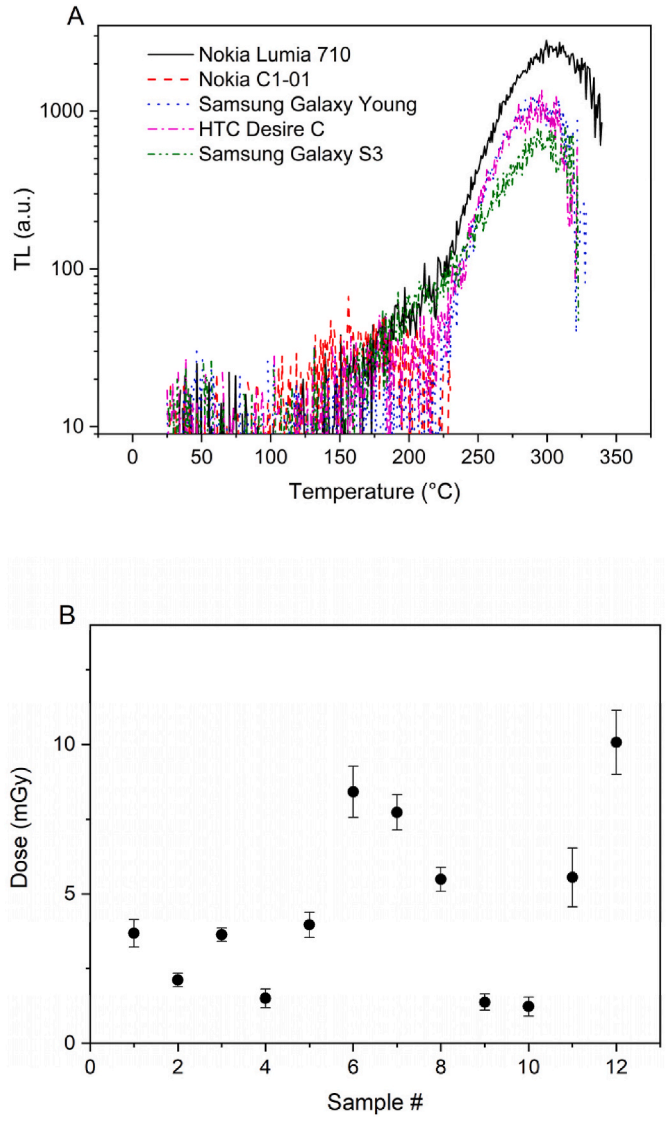

Fig. 7. Upper panel A: Zero-dose signals for selected samples. The number of measured resistors varies between samples as does the sensitivity per component. Lower panel B: Intrinsic background doses. To increase robustness in the results only the signal error was considered in the linear regression and for calculating the dose, although scatter of data points around calibration curve was generally larger than the pure signal error. Error bars in the figure therefore might underestimate the true uncertainty of the estimate. Sample code is: 1- Samsung Star 3; 2 - Nokia Lumia 710; 3 - Nokia C1-01; 4 - Samsung Galaxy Young; 5 - HTC Desire C; 6 - Nokia NPL-2; 7 - Nokia C1-01; 8 – Motorola; 9 - Samsung GT-S 5220; 10 - Samsung GT-S 5229; 11 – same model as 10; 12 – Samsung Galaxy S3.

kerma value. Doses measured using red TL of resistors, with either 4–5 resistors or using only a single resistor and corrected for fading using Fig. 12, lie within 25 % of the nominal dose value. Interestingly, all resistors samples from the LG model (no sensitization) show doses below the reference dose, whereas the aliquots from the Samsung model show doses above the reference dose. Part of the higher dose values for the latter samples may thus be ascribed to the de-sensitization during calibration (and possibly during measurement of the accident dose signal). Another source of uncertainty can also be a variability in fading rate, which could not be assessed in this study so far. From an empirical point of view, it is important to note that the dose method using red TL on resistors performs on an equal level as the dose assessment methods using other fortuitous materials (etched and unetched display glass) or protocols (OSL on resistors).

4. Summary and conclusions

Measurements and analysis of the TL and OSL emission spectra of the alumina substrates of resistors and inductors found on the circuit board of smartphones reveal the existence of three emission bands in the wavelength range relevant for PMT measurements. These are located between 320 and 330 nm, 410–430 nm and at 695 nm. The former two would be compatible with the emission characteristics of the F and F^+ centers in α-Al_2O_3, whereas the signal structure of the latter allows an unequivocal assignment to Cr^{3+} impurities. In the standard OSL configuration of many commercial luminescence readers, using blue LEDs for stimulation and a Hoya U-340 optical filter for detection, both emissions at 330 and 410 nm will always be measured but with different relative contributions. The TL spectra are dominated by the Cr^{3+} emission, with the peak intensity being almost a 100 times higher than the emissions in the blue/UV, in the case of resistors, confirming the

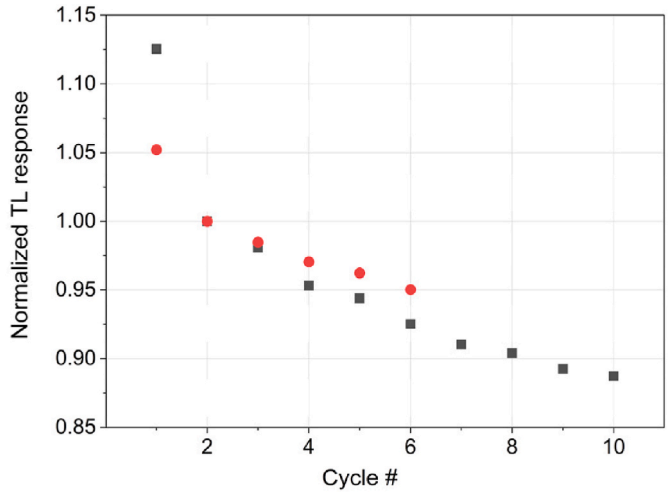

Fig. 8. Reproducibility test on two resistor samples, taken from two different Samsung Galaxy 3 phones (5 resistors each). Data are normalized to the TL response of the second cycle, to better visualize sensitivity changes after measurement of the accident signal (first cycle) and sensitivity changes during measurement of the dose calibration curve (second cycle onwards).

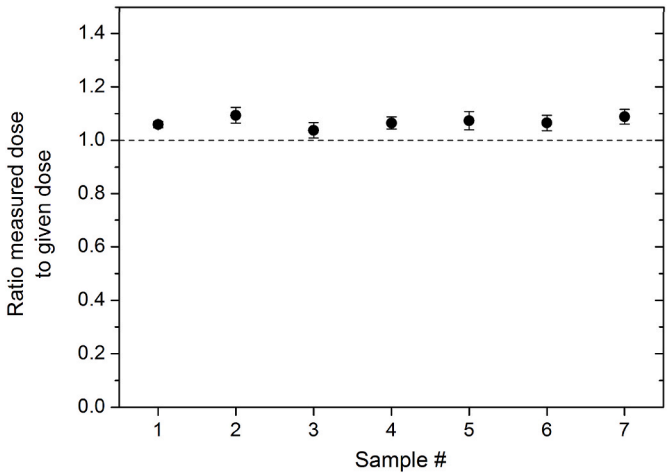

Fig. 9. Results of the dose recovery test on seven samples. Sample code is: 1 – Nokia NPL2; 2 - Nokia C1-01; 3 – Motorola; 4 - Samsung GT-S 5220; 5 - Samsung GT-S 5229; 6 – same model as 5; 7 – Samsung Galaxy S3. Average dose ratio with one standard deviation is 1.07 ± 0.02; average recycling ratio 0.94 ± 0.02.

findings of Lee et al. (2017). This can be caused by a higher impurity concentration, compared to the concentration of oxygen vacancies, and by the amplification of the Cr^{3+} emission by absorption of the 410 nm emission (and to a lesser degree also of the 330 nm emission).

Investigations of the dosimetric properties of the Cr^{3+} emission of resistors, using a red sensitive PMT and a longpass optical filter, show a similar glow curve shape, linear dose response, optical stability and fading characteristics as the blue/UV emission. This indicates that similar traps may be associated with all three recombination centers. Next to a significantly higher sensitivity, the red TL also shows the advantage of lower intrinsic background signals and corresponding apparent doses and less de-sensitization compared to blue TL, potentially enabling simpler measurement protocols. The irradiation trial has shown that the red TL method on resistors can compete in terms of accuracy with the dose assessment methods using other materials or protocols, even when using only a single resistor. In terms of radiation sensitivity, a detection limit below 1 mGy would be feasible, when using

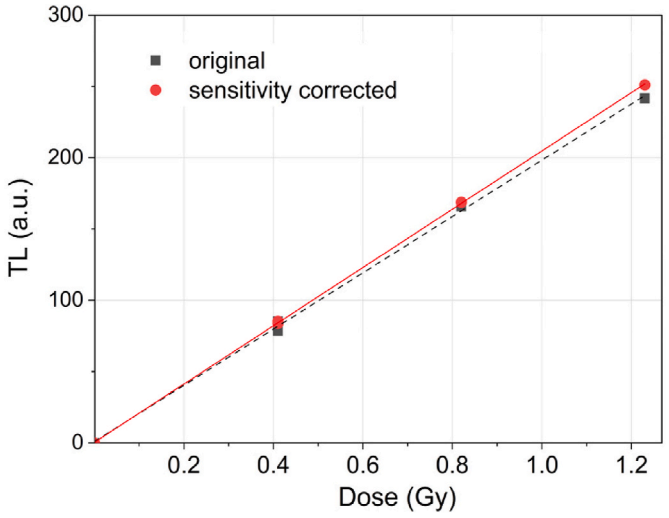

Fig. 10. Calibration curve of sample 5 from Fig. 9, without ("original") and with ("sensitivity corrected") correction using the data from Fig. 8.

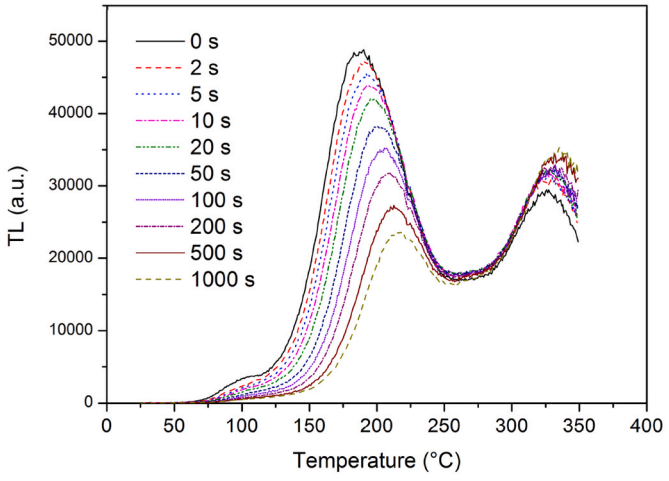

Fig. 11. Red TL using eight resistors, taken from a Nokia C1-01 phone, after irradiation with 4 Gy and different exposure times to blue LEDs (85 mW cm^{-2}). The time delay between irradiation and measurement was kept constant for all bleaching times. (For interpretation of the references to colour in this figure legend, the reader is referred to the Web version of this article.)

10 resistors, however the existence of the intrinsic background signals limits this value up to 10 mGy. Currently, the largest advantage of using red TL seems to be the possibility of doing dose reconstruction on a single resistor with the same sensitivity as blue TL or OSL when using 10 resistors. This theoretically opens the possibility to solder the resistor back in its original position on the circuit board after measurement and in this way to non-destructively measure the smartphone. It also offers a viable possibility for dose assessment when the number of available electronic components on the circuit board is limited in the first place and is not sufficient for blue TL or OSL, which can be the case for some modern smartphones or other smaller personal electronic devices. While the present study could demonstrate the potential of red TL of resistors for retrospective dosimetry more investigations are needed for improvements in sample preparation and protocols and performance assessment at lower doses.

CRediT authorship contribution statement

Clemens Woda: Writing – original draft, Visualization,

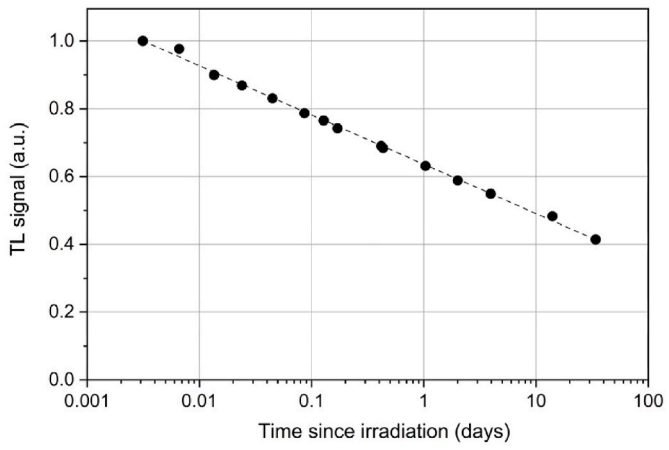

Fig. 12. Fading curve of the Cr^{3+} emission in resistors, measured for a cup of 5 resistors from LG P700. For t_C = 0.346 d (8.3 h), I_C = 0.703 and g = 20.7 % per decade.

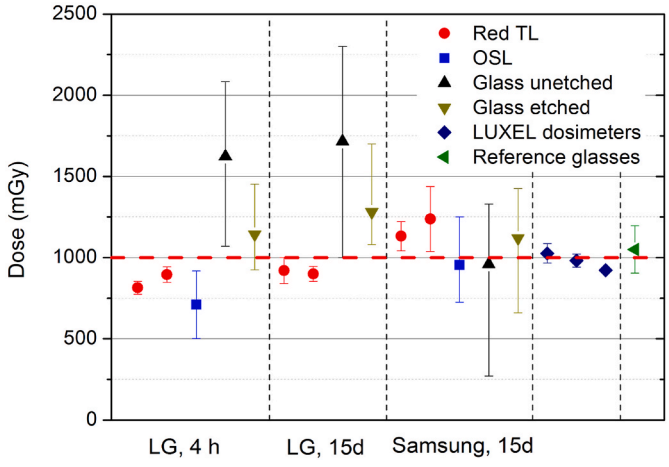

Fig. 13. Results of irradiation trial on two mobile phones (LG P700 and Samsung Galaxy Y) using resistors measured either with TL (Cr^{3+} emission) or OSL and using display glass (etched and unetched aliquots) measured with TL. The first datapoint for red TL per phone was measured using 4–5 resistors, the second using a single resistor. Time since irradiation is indicated behind the phone model name. Reference dosimeters (reference glasses and LUXEL detectors) were attached only to the Samsung phone. The LUXEL detectors are ordered from left to right according to their position on the phone (front, inside, back). (For interpretation of the references to colour in this figure legend, the reader is referred to the Web version of this article.)

Methodology, Investigation, Formal analysis, Conceptualization. **Michael Discher:** Writing – review & editing, Investigation, Conceptualization.

Funding sources

This research did not receive any specific grant from funding agencies in the public, commercial, or not-for-profit sectors.

Declaration of competing interest

The authors declare that they have no known competing financial interests or personal relationships that could have appeared to influence the work reported in this paper.

Acknowledgements

We are grateful to Freiberg Instruments GmbH for allowing test measurements on their equipment onsite for finding the optimal detector for the red TL measurements. We thank two reviewers, whose comments have significantly helped to improve the quality of the manuscript.

Data availability

Data will be made available on request.

References

Ademola, J.A., Woda, C., 2017. Thermoluminescence of electronic components from Mobile phones for determination of accident doses. Radiat. Meas. 104, 13–21.
Akselrod, M.S., Agersnap Larsen, N., Whitley, V., McKeever, S.W.S., 1998. Thermal quenching of F-center luminescence in Al2O3:C. J. Appl. Phys. 84, 3364–3373.
Bassinet, C., Le Bris, W., 2020. TL investigation of glasses from Mobile phone screen protectors for radiation accident dosimetry. Radiat. Meas. 136, 106384.
Bassinet, C., Trompier, F., Clairand, I., 2010. Radiation accident dosimetry on glass by TL and EPR spectrometry. Health Phys. 98, 400–405.
Bassinet, C., Woda, C., Bortolin, E., Della Monaca, S., Fattibene, P., Quattrini, M.C., Bulanek, B., Ekendahl, D., Burbidge, C.I., Cauwels, V., Kouroukla, E., Geber-Bergstrand, T., Mrozik, A., Marczewska, B., Bilski, P., Sholom, S., McKeever, S.W.S., Smith, R.W., Veronese, I., Galli, A., Panzeri, L., Martini, M., 2014. Retrospective radiation dosimetry using OSL of electronic components: results of an inter-laboratory comparison. Radiat. Meas. 71, 475–479.
Bassinet, C., Kreutzer, S., Mercier, N., Clairand, I., 2017. Violet stimulated luminescence signal from electronic components for radiation accident dosimetry. Radiat. Meas. 106, 431–435.
Bassinet, C., Discher, M., Ristic, Y., Woda, C., 2022. Mobile phone screen protector glass: a TL investigation of the intrinsic background signal. Front. Public Health 10.
Beerten, K., Woda, C., Vanhavere, F., 2009. Thermoluminescence dosimetry of electronic components from personal objects. Radiat. Meas. 44, 620–625.
Blasse, G., Grabmaier, B.C., 1994. Luminescent Materials, 1 ed. Springer, Berlin, Heidelberg, Heidelberg.
Discher, M., Woda, C., 2013. Thermoluminescence of glass display from Mobile phones for retrospective and accident dosimetry. Radiat. Meas. 53, 12–21.
Discher, M., Woda, C., Fiedler, I., 2013. Improvement of dose determination using glass display of Mobile phones for accident dosimetry. Radiat. Meas. 56, 240–243.
Discher, M., Bortolin, E., Woda, C., 2016. Investigations of touchscreen glasses from Mobile phones for retrospective and accident dosimetry. Radiat. Meas. 89, 44–51.
Discher, M., Woda, C., Ekendahl, D., Rojas-Palma, C., Steinhäusler, F., 2021. Evaluation of physical retrospective dosimetry methods in a realistic accident scenario: results of a field test. Radiat. Meas. 142, 106544.
Discher, M., Bassinet, C., Woda, C., 2023. A TL Study of Protective Glasses of Mobile Phones for Retrospective Dosimetry Optical Materials: X, 18, 100233.
Evans, B.D., Stapelbroek, M., 1978. Optical properties of the F+ Centre in crystalline Al2O3. Phys. Rev. B 18 (12), 7089–7098.
Fattibene, P., Trompier, F., Wieser, A., Brai, M., Ciesielski, B., De Angelis, C., Della Monaca, S., Garcia, T., Gustafsson, H., Hole, E.O., Juniewicz, M., Krefft, K., Longo, A., Leveque, P., Lund, E., Marrale, M., Michalec, B., Mierzwinska, G., Rao, J. L., Romanyukha, A.A., Tuner, H., 2014. EPR dosimetry intercomparison using smart phone touch screen glass. Radiat. Environ. Biophys. 53, 311–320.
Fiedler, I., Woda, C., 2011. Thermoluminescence of chip inductors from Mobile phones for retrospective and accident dosimetry. Radiat. Meas. 46, 1862–1865.
Geber-Bergstrand, T., Bernhardsson, C., Christiansson, M., Mattsson, S., 2018. Optically stimulated luminescence (OSL) dosimetry in irradiated alumina substrates from Mobile phone resistors. Radiat. Environ. Biophys. 57, 69–75.
Huntley, D.J., Lamothe, M., 2001. Ubiquity of anomalous fading in K-feldspars and the measurement and correction for it in optical dating. Can. J. Earth Sci. 38 (7), 1093–1106. https://doi.org/10.1139/e01-013.
Ibarra, A., Mariani, D.F., Jimenez de Castro, M., 1991. Thermoluminescent processes of $MgAl_2O_4$ irradiated at room temperature. Phys. Rev. B 41, 12158–12165.
Inrig, E.L., Godfrey-Smith, D.I., Khanna, S., 2008. Optically stimulated luminescence of electronic components for forensic, retrospective and accident dosimetry. Radiat. Meas. 43, 726–730.
Kim, H., Yu, H., Discher, M., Kim, M.C., Choi, Y., Lee, H., Lee, J.T., Lee, H., Kim, Y., Kim, H.S., Lee, J., 2022. A small-scale realistic inter-laboratory accident dosimetry comparison using the TL/OSL from Mobile phone components. Radiat. Meas. 150, 106696.
Kim, H., Kim, M.C., Van Hoey, O., Eakins, J.S., Yu, H., Lee, H., Discher, M., Lee, J., Waldner, L., Woda, C., Trompier, F., Bassinet, C., Sholom, S., McKeever, S.W.S., Ainsbury, E.A., 2025. Monte Carlo dosimetry for a EURADOS WG 10 and RENEB field test of retrospective dosimetry techniques in realistic exposure scenarios. Radiat. Meas. 180, 107329.
Lee, J.I., Kim, H., Kim, J.L., Pradhan, A.S., Kim, M.C., Chang, I., Lee, S.K., Kim, B.H., Park, C.Y., Chung, K.S., 2017. Thermoluminescence of chip inductors and resistors in new generation Mobile phones for retrospective accident dosimetry. Radiat. Meas. 105, 26–32.

McKeever, S.W.S., Akselrod, M.S., Colyott, L.E., Agersnap Larsen, N., Polf, J.C., Whitley, V., 1999. Characterisation of Al_2O_3 for use in thermally and optically stimulated luminescence dosimetry. Radiat. Protect. Dosim. 84, 163–168.
McKeever, S.W.S., Minniti, R., Sholom, S., 2017. Phototransferred thermoluminescence (PTTL) dosimetry using gorilla® glass from Mobile phones. Radiat. Meas. 106, 423–430.
Mrozik, A., Marczewska, B., Bilski, P., Klosowski, M., 2014. Investigation of thermoluminescence properties of Mobile phone screen displays as dosimeters for accidental dosimetry. Radiat. Phys. Chem. 104, 88–92.
Mrozik, A., Marczewska, B., Bilski, P., Ksiazek, M., 2017. OSL signal of IC chips from Mobile phones for dose assessment in accidental dosimetry. Radiat. Meas. 98, 1–9.
Richter, D., Richter, A., Dornich, K., 2013. Lexsyg — a new system for luminescence research. Geochron 40, 220–228.
Rojas Palma, C., Woda, C., Discher, M., Steinhäusler, F., 2020. On the use of retrospective dosimetry to assist in the radiological triage of mass casualties exposed to ionizing radiation. J. Radiol. Prot. 40, 1286–1298.
Sholom, S., McKeever, S.W.S., 2016. Integrated circuits from Mobile phones as possible emergency OSL/TL dosimeters. Radiat. Protect. Dosim. 170, 398–401.
Waldner, L., Bernhardsson, C., Woda, C., Trompier, F., Van Hoey, O., Kulka, U., Oestreicher, U., Bassinet, C., Rääf, C., Discher, M., Endesfelder, D., Eakins, J.S., Gregoire, E., Wojcik, A., Ristic, Y., Kim, H., Lee, J., Yu, H., Kim, M.C., Abend, M., Ainsbury, E., 2021. The 2019-2020 EURADOS WG10 and RENEB field test of retrospective dosimetry methods in a small-scale incident involving ionizing radiation. Radiat. Res. 195, 253–264.
Woda, C., Greilich, S., Beerten, K., 2010. On the OSL curve shape and preheat treatment of electronic components from portable electronic devices. Radiat. Meas. 45, 746–748.
Yukihara, E.G., McKeever, S.W.S., 2011. Optically Stimulated Luminesence. Fundamentals and Application. Wiley & Sons Ltd.